Fermi National Accelerator Laboratory

FERMILAB-Conf-95/189-E
D0

D0 Top Quark Mass Analysis

M. Strovink
For the D0 Collaboration

Fermi National Accelerator Laboratory
P.O. Box 500, Batavia, Illinois 60510

University of California and Lawrence Berkeley Laboratory
Berkeley, California 94720

July 1995

To be published in the Proceedings *10th Topical Workshop on Proton-Antiproton Collider Physics*, Fermi National Accelerator Laboratory, Batavia, Illinois, May 9-13, 1995

Disclaimer

DØ Top Quark Mass Analysis

M. Strovink for the DØ Collaboration[1]

University of California and Lawrence Berkeley Laboratory
Berkeley, California 94720

Fermi National Accelerator Laboratory, Batavia, Illinois 60510
(June 28, 1995)

Based on (44-48 pb^{-1}) of lepton + jets data, we review DØ's initial analysis of the top quark mass. The result, $M_{\rm top} = 199^{+19}_{-21}$ (stat.)$\pm$22 (syst.) GeV/c^2, is insensitive to background normalization. The errors are based on ISAJET top Monte Carlo, with its more severe gluon radiation, and allow for ISAJET/HERWIG differences. Good progress is being made in reducing the systematic error.

We present a new study based on two-dimensional distributions of reconstructed top quark *vs.* dijet mass. With 98.7% confidence we observe a peak in the top mass - dijet mass plane. The peak and its projections are similar both in shape and magnitude to expectations based on the decay sequence $t \to bW$, $W \to jj$.

INTRODUCTION AND PRELIMINARIES

As an essential part of DØ's published (1) observation of the top quark, our initial analysis of the top quark mass was described. Here we review that work and present a new M_t-M_{jj} study based on two-dimensional distributions of reconstructed top *vs.* dijet mass.

This report is based on DØ's February 1995 (44-48 pb^{-1}) lepton + jets data sample and event selection criteria, which are reviewed elsewhere (2) in these Proceedings. By default, loose cuts are applied. They differ from standard DØ cuts in that the multijet aplanarity requirement $\mathcal{A} > 0.05$ is relaxed to $\mathcal{A} > 0.03$, and the cut on multijet scalar E_T ($H_T > 200$ GeV) is released altogether. Taking advantage of reduced mass bias and larger acceptance, the loose cuts permit a better top quark mass measurement than do the standard cuts despite admitting more background.

To be analyzable for top quark mass, an event must include four jets (b,b,j,j) with $E_T >$ 15 GeV, an electron or muon (l) with $p_T > 20$ GeV/c for electrons and 15 GeV/c for muons, and missing $E_T > 20$ GeV (25 GeV for $l \equiv e$ with no soft muon tag). The jet E_T threshold is the same as for standard event selection; no jets already discarded because of low E_T are rescued for purposes of mass analysis. The four highest E_T jets with pseudorapidity $|\eta| < 2.5$ are presumed to arise from $t\bar{t}$ decay; at present any others are ignored.

From these ingredients, after solving for both neutrino longitudinal momenta consistent with $m(l\nu) = M_W$, one may reconstruct eight distinct pairs of top quark masses $\{m(bl\nu), m(bjj)\}$. If a soft muon tags one jet as a b, the number of possible pairs is halved. In our published (2C) top quark mass analysis, we impose the two constraints $m(bl\nu) = m(bjj)$ and $m(jj) = M_W$. When the jets are assigned correctly, this sharpens the

[1]To be published in the Proceedings, 10th Topical Workshop on Proton-Antiproton Collider Physics, Fermilab, Illinois, 9-13 May 1995.

mass resolution. However, forcing $m(jj) = M_W$ triples the number of distinct top quark mass pairs which must be considered.

JET CORRECTIONS

Ambiguities involving the assignment of jets and the role of initial and final state radiation (ISR and FSR) must carefully be taken into account. For this we use a Monte Carlo (MC) template method. In this method, data and MC are processed by the same algorithm to yield distributions in one or more variables, *e.g.* the apparent top quark mass. These distributions are then compared, and the true top quark mass input to the MC is varied to optimize their consistency. Thus the most important quantity to be calibrated is the *relative* energy of jets in the data and MC. Absolute energy calibration is a lesser but not a negligible goal, since it affects the resolution with which the apparent and true top quark masses are related.

At present, DØ jets are clustered using a cone algorithm. We use cones with $\mathcal{R} = 0.5$ for event selection and M_t-M_{jj} analysis, and with $\mathcal{R} = 0.3$ for 2C top quark mass analysis. In the initial stage of calibration, detector dependent corrections are made for calorimeter energy response, for spreading in the calorimeter of showers out of and into the cones, and for underlying events. The first correction is the largest. The calorimeter's electromagnetic (EM) energy component is calibrated using $Z \rightarrow ee$, $J/\psi \rightarrow ee$, and $\pi^0 \rightarrow \gamma\gamma$ peaks from the data. The hadronic energy component is referenced to the EM component by studying transverse energy balance in final states consisting of one hadron jet and one EM object (3). The Monte Carlo calorimeter energy is calibrated using an identical procedure based on fully simulated calibration data. Typically the hadronic energy correction for the sum of detector dependent effects is +20%.

The result of this initial calibration stage is a set of cone jets from which detector dependent energy biases in principle have been removed. Their energy calibration is checked by making 1C fits to single jet + ($Z \rightarrow ee$) data in which the minimum jet E_T is 20 GeV. Figures 1(a) and (b) display the transverse energy balance from such fits to Monte Carlo and data events. The relative agreement is good, but both peaks are displaced from zero because parton fragments outside the cone ($\mathcal{R} = 0.3$ there) do not contribute to the cone jet energies, affecting the absolute energy calibration.

In the final calibration stage, based on Monte Carlo studies of jet *vs.* parton energies in top quark final states, $\mathcal{R} = 0.3$ cone jet transverse energies are multiplied by $\approx$1.08 and also increased by $\approx$5 GeV to account for these out-of-cone effects. The out-of-cone corrections for b and lighter quark jets are nearly the same (4). Figures 1(c) and (d) show the improvement in transverse energy balance once this final correction is made. The out-of-cone corrections to jets with $\mathcal{R} = 0.5$ are smaller; they are not applied in the M_t-M_{jj} analysis.

Lastly, if a jet in a top candidate event is tagged by a soft muon, twice the tag muon momentum is added to its energy to account for the energy, undetected in the calorimeter, of both the tag muon and, on average, its associated neutrino. From the Z+jet studies we estimate that the relative miscalibration of jet energies in data and MC is 10% or less.

2C MASS ANALYSIS

In DØ's 2C mass analysis, all possible solutions [totalling 12 (24) if a soft muon tag is (is not) present] are subjected to a true two constraint fit (5). At present the fitted

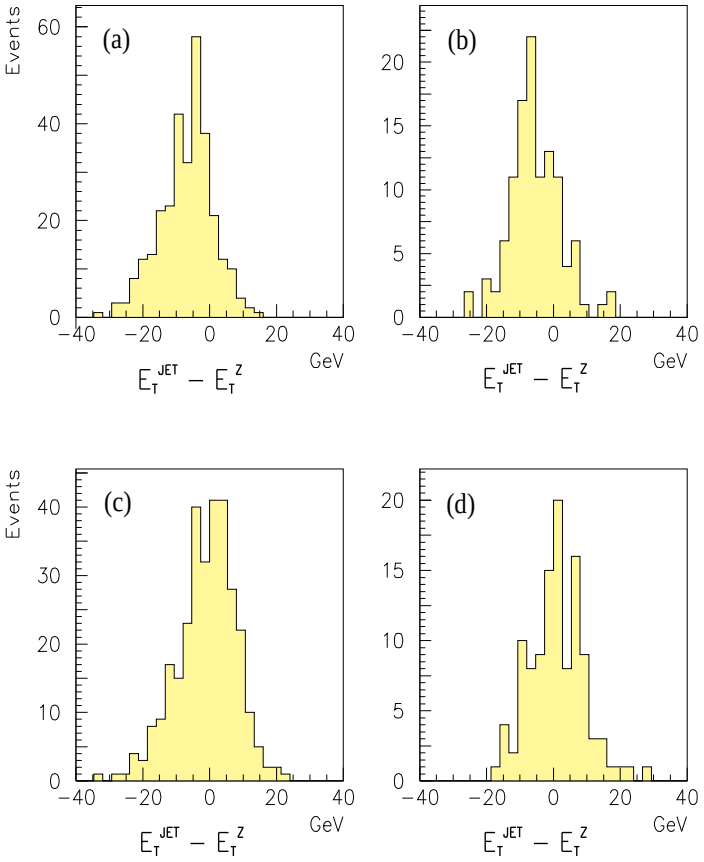

FIG. 1. Difference between reconstructed $\mathcal{R} = 0.3$ cone jet transverse energy and recoiling $Z \to ee$ transverse energy in Z + single jet events, for (a,c) Monte Carlo and (b,d) data. In (c) and (d) only, out-of-cone corrections to the jet energies are applied.

top quark mass is taken to be the average, weighted by $\exp(-\chi^2/2)$, of top masses from up to three best (6) 2C fits with $\chi^2 < 7$. Taking such an average is motivated primarily by sparse candidate statistics: if only the single best solution were chosen, small changes *e.g.* in jet energy calibration could interchange the χ^2 rank of two best solutions having widely different fitted top quark masses, causing a significant discontinuity in the overall result.

Lineshapes

The resulting resolution lineshapes for ISAJET (7) top events of various masses, passed through a GEANT (8) simulation of the DØ detector and the full DØ reconstruction machinery, are shown in Fig. 2(a)-(e). Also displayed in Fig. 2(f) is the soft fitted top mass spectrum from the dominant W+jets background, simulated by VECBOS (9) W + four jet Monte Carlo, with additional gluon radiation and fragmentation supplied by ISAJET. (A

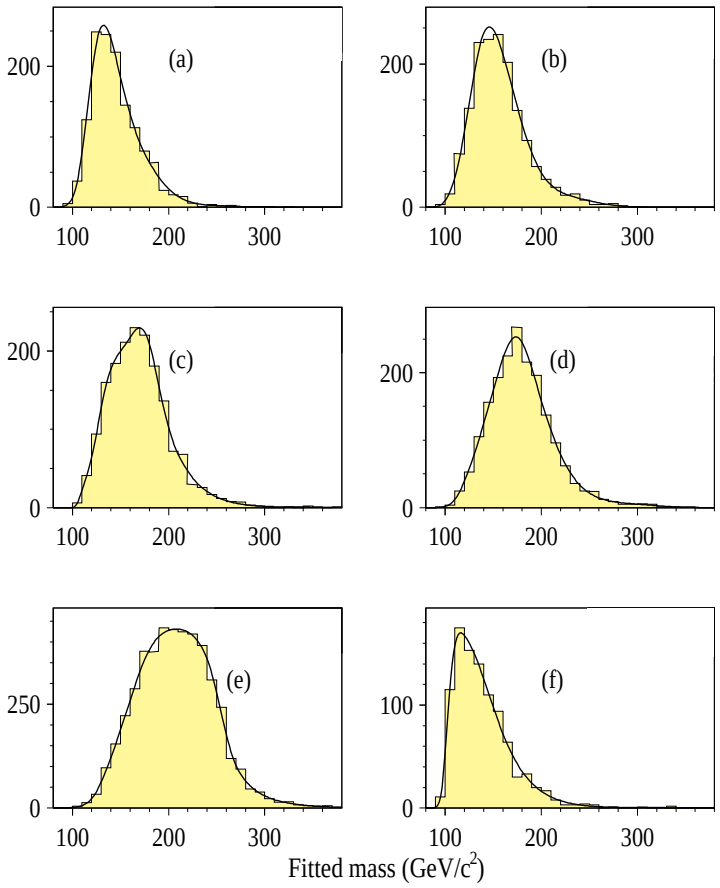

FIG. 2. Distributions of 2C fitted top quark mass for ISAJET Monte Carlo with input top masses of (a) 140, (b) 160, (c) 180, (d) 200, and (e) 240 GeV/c^2; and (f) for VECBOS W + four jet Monte Carlo.

smaller background component from QCD multijets is also present; it has a harder spectrum of fitted top mass. The QCD component is added to the Fig. 2(f) spectrum to obtain the background lineshape used in the fits.)

The mean fitted top quark mass grows with the true mass, as exhibited in Fig. 3(a), but the two variables are only ≈60% correlated. This incomplete correlation is a basic feature of lepton + jets top final states. It is caused by the effects of wrong jet assignment, of ISR especially at low true top quark masses, and of FSR especially at high true top masses. For use in further analysis, these lineshapes are smoothed and parametrized as a continuous function of true top mass, as shown in Fig. 3(b).

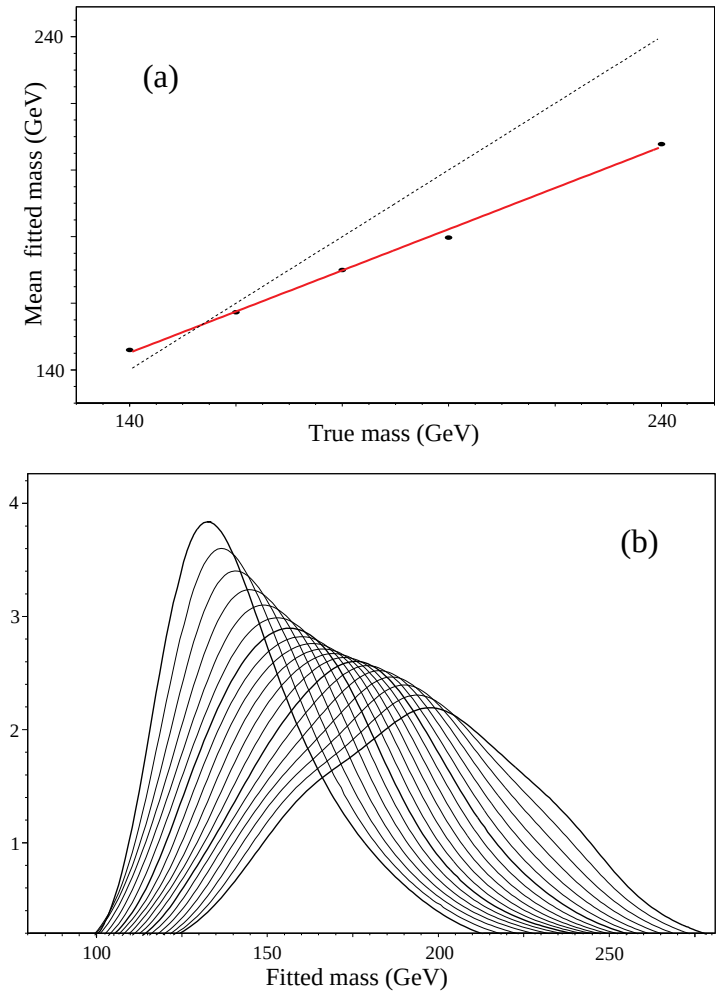

FIG. 3. (a) Mean fitted *vs.* input ISAJET Monte Carlo top quark mass (y *vs.* x). The solid line, fitted to the points, satisfies the equation $y = 58.6 + 0.62\,x$. The dotted line satisfies $y = x$. (b) Smoothed and interpolated distributions of fitted top quark mass for input ISAJET Monte Carlo top masses in 5 GeV/c^2 steps. The bold curves denote input masses of 140, 170, 200, and 230 GeV/c^2, respectively.

Varying the MC Generator

The effects of initial and final state radiation are more severe for ISAJET top quark Monte Carlo than for HERWIG (10), as illustrated in Fig. 4. Consider first the histograms in Figs. 4(a) and (b). The subsets of (a) ISAJET and (b) HERWIG Monte Carlo 180 GeV/c^2 top events plotted there contain exactly four detected jets within cuts; each jet is associated uniquely with each of the four primary jets (two b jets and two W jets) required for mass analysis. For the shaded data the jets are assigned in the 2C fit by cheating, *i.e.* by using the Monte Carlo information. With these simplifications, the widths of the shaded histograms arise mainly from detector resolution and undetected FSR. If instead the best jet assignment

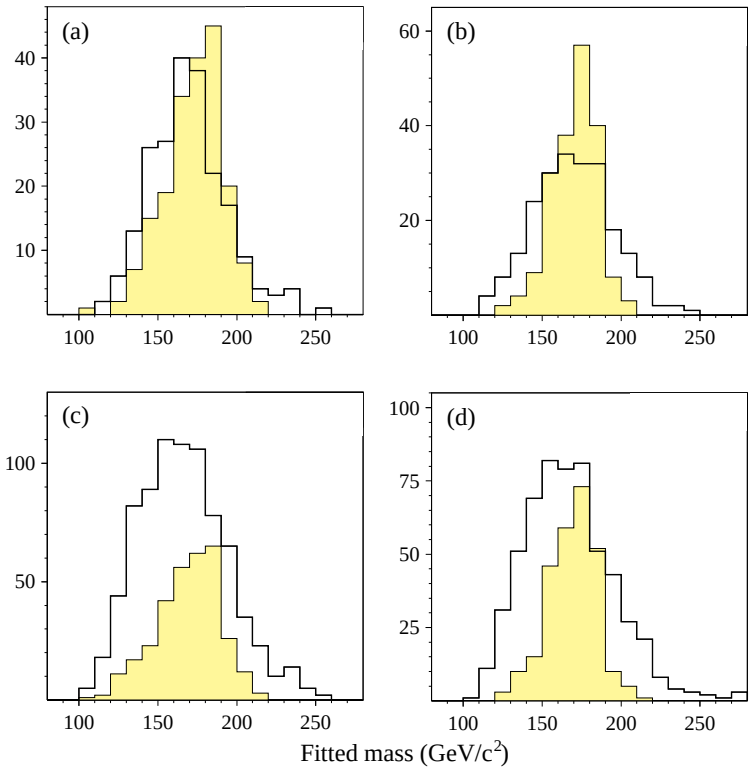

FIG. 4. Distributions of fitted top quark mass for (a,c) ISAJET and (b,d) HERWIG 180 GeV/c^2 top Monte Carlo. In (a) and (b), events have exactly four detected and accepted jets, uniquely matched to the four primary jets (two b jets + two W jets) required for mass analysis. In (b) and (d), four or more detected and accepted jets are allowed as in actual analysis, without any matching requirement. Open histograms show the fitted top quark mass as in actual analysis. Shaded histograms, which are filled only for those events in which the four highest E_T jets are uniquely matched to the four primary jets, show the 2C fit mass for the correct jet assignment.

is chosen based on minimum χ^2 (*i.e.* without cheating), the open histograms are obtained. There the additional broadening due to jet misassignment is evident.

In contrast, the data plotted in Figs. 4(c) and (d) simply require at least four jets satisfying the cuts, without any association requirement. This reflects actual analysis. With these less stringent requirements, often one of the four highest E_T jets is ISR or FSR. Cheating is possible only in the complementary case in which the four highest E_T jets are matched uniquely to each of the primary jets. Here the differences between (c) ISAJET and (d) HERWIG are more evident. Compared to HERWIG, the information needed to make a correct fit is available less frequently for ISAJET events. Without and especially with cheating, the more severe FSR in the ISAJET data causes prominent low tails in the lineshapes.

In its 2C mass analysis, DØ approaches this problem by quoting statistical and systematic errors based on ISAJET, for which the effects of gluon radiation are more severe. We include

in the systematic error an allowance for the difference in MC generators.

Likelihood Fit

Of the 29 lepton + jets events surviving loose cuts, 27 have four jets passing the usual jet cuts and 24 have at least one 2C fit with $\chi^2 < 7$. Taking into account the efficiency for yielding a good 2C fit, the background determined from the counting experiment (1) is $N_b = 11.6 \pm 2.2$ events.

We perform an unbinned Poisson-statistics maximum likelihood fit to the true top quark mass $M_{\rm top}$ using the straightforward method and notation introduced by CDF (11). The unknowns are $M_{\rm top}$ and the expected number n_s (n_b) of signal (background) events. Within its gaussian error, N_b externally constrains n_b. The top MC mass distributions are as in Fig. 2(a)-(e); the background is determined from the counting experiment (1) to be 70% VECBOS W + four jets as in Fig. 2(e) and 30% QCD multijet fakes as measured from data not satisfying one or more of the standard electron identification criteria.

We have studied the behavior of this fitting method using ensembles of simulated data samples consisting of $N/2$ background and $N/2$ top quark events with generated mass M. The cases $N = 24$ and $N = 200$ are exhibited in Fig. 5(a)-(d) for $M = 160$ and 200 GeV/c^2. These ensemble studies confirm that the maximum likelihood $M_{\rm top}$ reproduces the input M to within ± 4 GeV/c^2, and that the statistical error decreases nearly as $1/\sqrt{N}$. Figure 5(e) encourages us to expect for our conditions a statistical error on $M_{\rm top}$ in the range $\approx$ 12-25 GeV/c^2, with a most likely value of 16 GeV/c^2.

Results of 2C Mass Fit

Figures 6(b) and (d) exhibit the results of the maximum likelihood fit. In Fig. 6(b) the dashed line is the distribution in fitted top quark mass for the sum of W+jets and QCD multijet fake background, while the dotted line is the lineshape for the best fit $M_{\rm top} = 199^{+19}_{-21}$ (stat.) GeV/c^2. Their areas correspond to $n_b = 11.6^{+2.0}_{-2.0}$ and $n_s = 12.3^{+5.0}_{-4.2}$ events respectively. The sum of these curves (solid line) clearly is an excellent fit to the data. None of the variables n_s, n_b, $M_{\rm top}$, and the statistical error on $M_{\rm top}$ change significantly when the external constraint on n_b is lifted. For example, the unconstrained best fit background is $n_b = 11.8^{+5.8}_{-5.2}$ (stat.)

If HERWIG were substituted for ISAJET, $M_{\rm top}$ would decrease by 4 GeV/c^2 and its statistical error would decrease by 19%. Also shown in Fig. 6(a) and (c) is a similar fit to the standard cut data, yielding the same central $M_{\rm top}$ and larger errors.

DØ's published (1) ± 22 GeV/c^2 systematic error on $M_{\rm top}$ is dominated by the 10% jet energy scale error discussed above. This was evaluated simply by varying the jet energies by $\pm 10\%$ and dividing the resulting shift in the fitted top quark mass by the slope of the mean fitted mass *vs.* true top mass (Fig. 3(a)).

In a refined procedure, we repeat the ensemble of Monte Carlo experiments after jet energies are varied by $\pm 10\%$ in both the 200 GeV/c^2 top and W+jets components of the simulated data samples. The mean maximum likelihood top quark masses are 177, 197, and 209 GeV/c^2 for jet energy scales which are 90%, 100%, and 110% of nominal, respectively, yielding a scale error of $^{+12}_{-20}$ GeV/c^2.

In addition to the jet scale error, the current systematic error in top quark mass includes ± 4 GeV/c^2 from the HERWIG/ISAJET difference; ± 4 GeV/c^2 from differences observed in

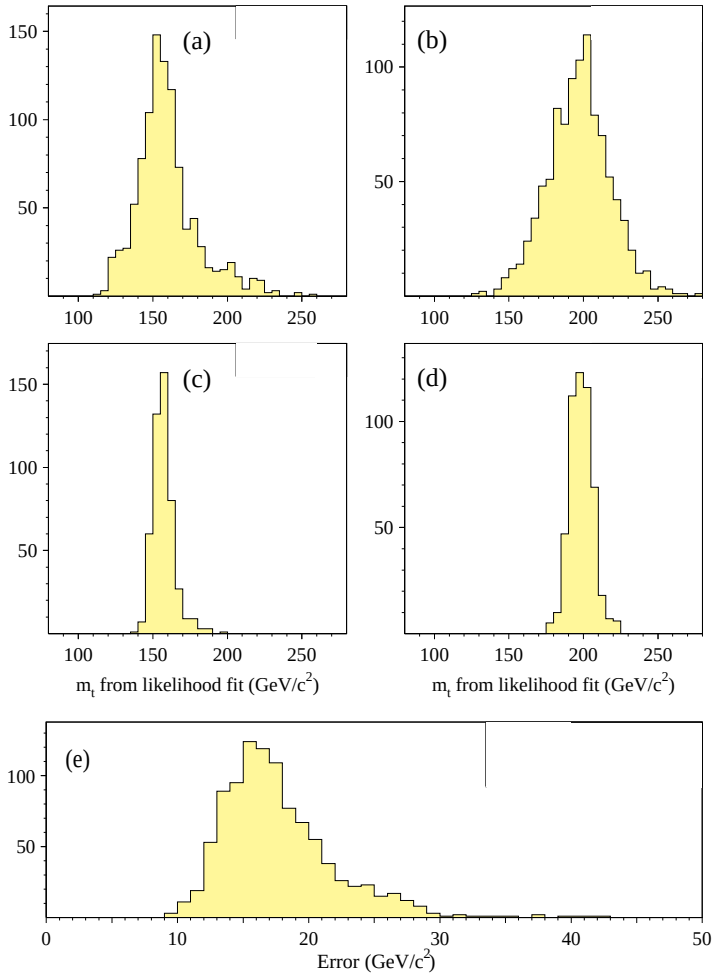

FIG. 5. Distributions from studies of ensembles of $N/2$ background events + $N/2$ ISAJET Monte Carlo events generated with top quark mass M. For (a) and (c) $M = 160$ GeV/c^2, while for (b), (d), and (e) $M = 200$ GeV/c^2; for (a), (b), and (e) $N = 24$ events, corresponding to the loose cut data sample, while for (c) and (d) $N = 200$ events. (a-d) display distributions of maximum likelihood fit true top mass m_t; (e) is the distribution of the statistical error on m_t from the likelihood fit.

ensemble tests between best fit and true top masses; ± 2 GeV/c^2 from varying the QCD multijet fake background fraction; and ± 5 GeV/c^2 from variations in the background shape and other sources. The quadrature sum yields a total systematic error of $^{+14}_{-21}$ GeV/c^2. Were HERWIG substituted for ISAJET, the systematic error would become $^{+13}_{-19}$ GeV/c^2. Work continues to further reduce these errors.

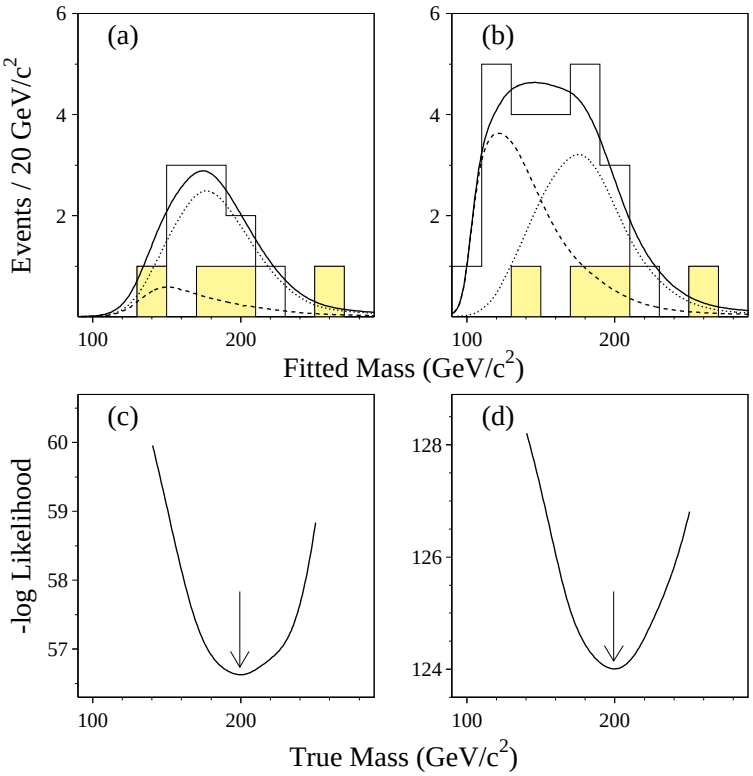

FIG. 6. (a,b) Histogram of fitted top quark mass for (a) standard cut and (b) loose cut data. The dotted curve shows the distribution of fitted mass for the maximum likelihood true mass of 199 GeV/c^2; the dashed curve displays the background distribution normalized to its maximum likelihood area; the solid curve is the sum. (c,d) -ln likelihood *vs.* true top mass for (c) standard cut and (d) loose cut data.

RECONSTRUCTED TOP VS. DIJET MASS STUDY

The statistical significance of DØ's top quark signal is established by its published (1) counting experiment. There we also display a clear excess of events having large trijet mass and minimum dijet mass compared to expected background. DØ's loose cut 2C top quark mass analysis, reviewed above, obtains a top mass lineshape which is different from that of expected background. As just noted, the top quark mass determined in the 2C likelihood analysis is essentially unchanged if the constraint on background normalization is removed. This supports the background calculation used by the counting experiment.

These points having been established, we reexamine the reconstructed top and dijet masses with the questions: Does DØ see a $W \rightarrow jj$ mass peak in its top quark sample? If so, are the top and W mass peaks correlated? Can the top mass be calibrated against the W mass in the same final state? *Preliminary* analysis described here will be sufficient to address the first two questions.

M_t-M_{jj} Analysis Method

Since no $m(jj) = M_W$ constraint should be applied when the dijet mass itself is studied, we are blessed with only 4 (8) distinct pairs $\{m(bl\nu), m(bjj)\}$ when a soft muon tag is (is not) present. Half of these involve the larger of two possible neutrino longitudinal momenta. These solutions are less likely than their complements and are rejected. The remaining two or four solutions are weighted according to $\exp(-\chi^2/2)$ with $\chi^2 \propto \ln^2(m(bl\nu)/m(bjj))$. Each event's weights are normalized in order to sum to unity.

For the reconstructed top quark mass M_t we plot the weighted average (12) of $m(bl\nu)$ and $m(bjj)$. For the dijet mass M_{jj}, when the b jet from $t \to bjj$ is untagged, often we assign the b to jet 1 (the most energetic in the top CM) and correspondingly plot m_{23}. But if $(E_1 - E_2) < (E_2 - E_3)$ in that frame, instead we plot both m_{23} and m_{13} with equal weight. We emphasize that dijet energies are *not* varied, and dijets are *not* selected for consistency with M_W.

When applied to 200 GeV/c^2 HERWIG top quark Monte Carlo, this analysis method yields the Lego plot and its projections shown in Fig. 7. A clear peak in both reconstructed top and dijet mass is evident. The top mass projection is slightly broader than that obtained by the 2C fit in Fig. 2(d). When the true top quark mass is varied, the slope like that displayed in Fig. 3(a) is slightly steeper. The reconstructed top and dijet mass peaks are close to the true top and W masses, respectively; the peak widths scale roughly as $\sqrt{m}$. Varying the true top mass does not substantially move the dijet mass at which the peak occurs, but the wings of the dijet distribution do change.

When applied to the above described combination of VECBOS W + four jets and QCD multijet fake background, the same analysis yields the quite different Lego plot in Fig. 8(b). There the peak appears at much smaller values of top and dijet mass. Also shown in Fig. 8(a) is the expected sum of 200 GeV top signal and background, with top normalized to the signal (=11.1) obtained by subtracting calculated background from the number of events observed in the counting experiment (2). The top quark signal appears as a prominent shoulder connected to the background peak.

M_t-M_{jj} Results

Figure 9 displays projections on the reconstructed top and dijet mass axes of the data. From Fig. 8(a) we expect the full projections to be dominated by background. This is avoided in Fig. 9 by projecting dijet masses only for reconstructed top masses exceeding 150 GeV/c^2, and by projecting reconstructed top masses only for dijet masses exceeding 58 GeV/c^2. Shown for comparison are the same projections for the expected combination of signal and background, and for background alone.

Subject to the statistical probabilities discussed below, we interpret the reconstructed top mass projection in Fig. 9(a) as evidence for a top quark mass peak. The data are distributed in the shape of a peak, in agreement with expectation. In contrast the background is smaller in magnitude relative to the expected $t\bar{t}$ component; it is shifted and dissimilar in shape. Likewise, we interpret the dijet mass projection in Fig. 9(b) as evidence for a W mass peak. Again the data are peaked, as is the expected combination of signal and background. Again the background is smaller in magnitude than for $t\bar{t}$; it is much broader in shape.

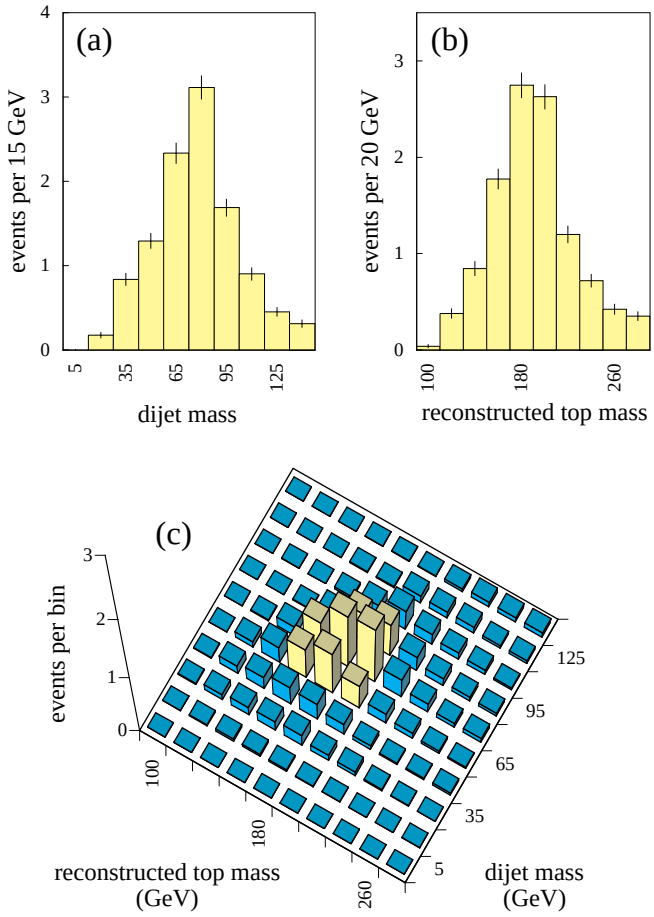

FIG. 7. (a,b) Projections and (c) Lego plot of HERWIG 200 GeV/c^2 top Monte Carlo events *vs.* reconstructed top mass and dijet mass. The plots contain 1868 events, which are normalized to the number (11.1) of loose cut top events obtained from the counting experiment. The mean projected masses are (a) 77 and (b) 190 GeV/c^2; the standard deviations are (a) 25 and (b) 35 GeV/c^2.

Significance of Peak

Were the discussion to terminate at this point, two essential questions would be left unaddressed. Do the same candidate events which contribute to the top peak also contribute to the W peak? If so, is the correlated peak statistically significant?

Figure 10 presents the Lego plot of the data. It confirms that the top and W peaks indeed arise mainly from the same events. The data are very different from the background (Fig. 8(b)); they are *not* very different from the expected combination of background and top quark signal (Fig. 8(a)). If anything, the M_t-M_{jj} peak in the data appears to be slightly better separated from the background than would be expected.

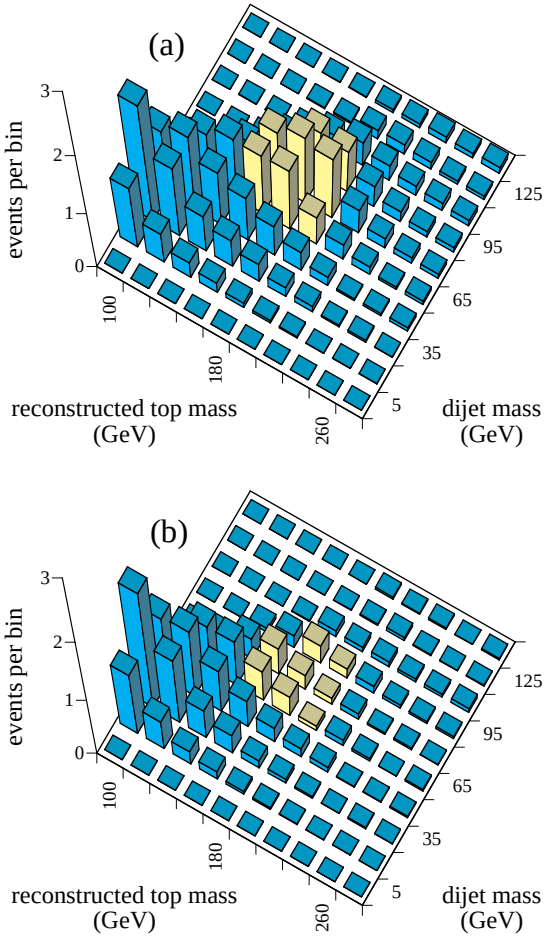

FIG. 8. Lego distributions in reconstructed top quark mass and dijet mass of (a) sum of HERWIG 200 GeV/c^2 top Monte Carlo and background events; (b) background alone. The background includes both W + four jet VECBOS Monte Carlo and QCD multijet data, each normalized using control samples.

As for statistical significance, we are concerned not simply with assessing the extent to which the data are inconsistent with background alone. That question does not directly address the existence of a *peak* in top and W mass. Rather, we return to the expected signal and background in Figs. 7(c) and 8(b) to calculate the ratio ρ of expected signal to the square root of expected signal + background for those data. This provides an objective, data-independent definition of the peak region. The Lego distribution of ρ is displayed in Fig. 11(b), where the light shaded cluster of eight highest bins defines the peak region (this shading appears also in the other Lego plots).

Recall that each event, with its multiple solutions, can increment more than one Lego bin. The sizes of these increments are determined by the extent to which $m(bl\nu)$ and $m(bjj)$ agree. For each event the increments sum to unity. We calculate the fraction f of each

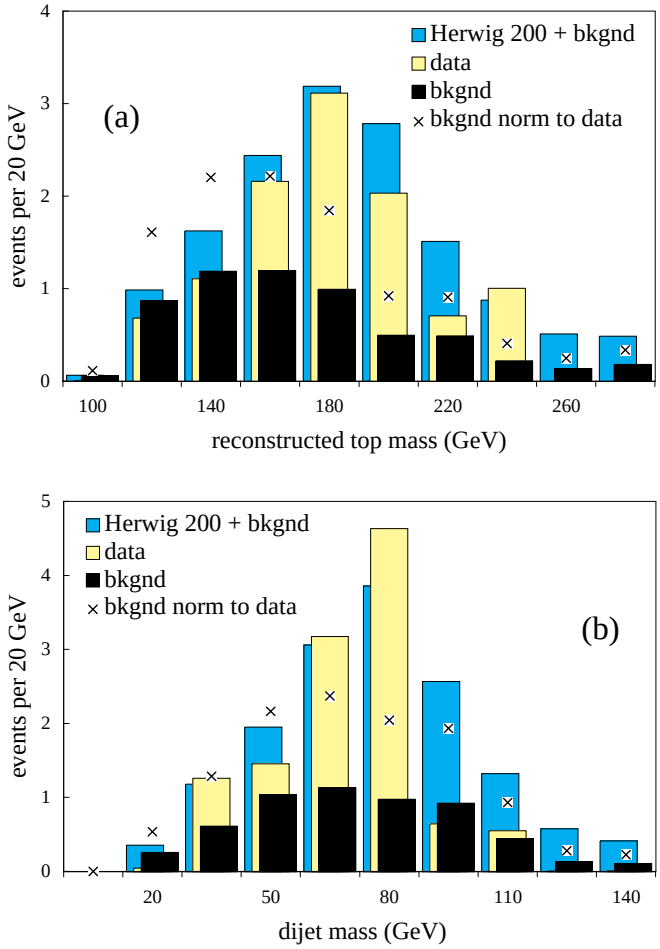

FIG. 9. Distributions of (a) reconstructed top quark mass M_t and (b) dijet mass M_{jj} with (a) $M_{jj} > 58$ GeV/c^2 and (b) $M_t > 150$ GeV/c^2, for (light shaded) data, (medium) sum of background and HERWIG 200 GeV/c^2 top Monte Carlo, (black) background alone, and (X's) background normalized to match the area of the data.

event's total increment which is allocated to the peak region. Figure 11(a) presents the distribution of f for data, for expected background, and for top Monte Carlo. Most of the background events have $f < 0.1$, *i.e.* devote less than 10% of their probability to the peak region. Most of the MC top events are broadly distributed up to $f = 1$. The data are intermediate. Fourteen candidates have $f < 0.1$. Twelve devote significant probability to the peak region; four concentrate $> 80\%$ of their probability there.

The distributions in Fig. 11(a) contain integral numbers of events, in contrast to those in Figs. 7-10. This permits a binned Poisson-statistics maximum likelihood fit (13) to their shapes in order to determine the fraction of the data which are consistent with top. For this fraction we obtain $0.43^{+0.23}_{-0.20}$, in excellent agreement with the counting experiment value for the same sample, 0.38 ± 0.21. If the top fraction is forced to zero, the likelihood decreases

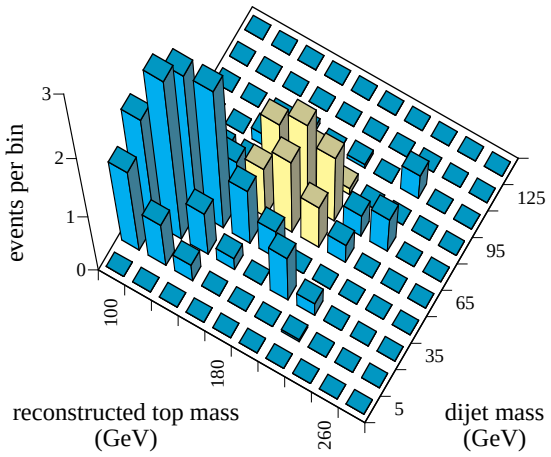

FIG. 10. Lego distribution in reconstructed top quark mass and dijet mass of the data (26 events). The events usually increment more than one bin because of multiple solutions; the increments for each event are normalized so that they sum to unity.

by an amount corresponding to a gaussian excursion of 2.2 standard deviations. A single-sided fluctuation of equal or greater magnitude is 1.3% probable. Since the Fig. 11(a) distributions are comparable for the two types of background, and the absolute rates are irrelevant to this fit, no significant systematic uncertainty in this fit top fraction is present.

CONCLUSIONS

We have published a 2C lepton+jets top quark mass analysis. The maximum likelihood fit result

$$M_{\rm top} = 199^{+19}_{-21}\,({\rm stat.}) \pm 22\,({\rm syst.})\,{\rm GeV}/c^2$$

is insensitive to background normalization. Errors are (conservatively) based on ISAJET and allow for ISAJET/HERWIG differences. Both the data and Monte Carlo jet energy scales have been cross-checked using constrained fits to single jet plus $Z \to ee$ final states; the assigned jet energy scale error reflects the accuracy of that check. Good progress is being made in reducing the systematic error.

We have presented new distributions of reconstructed top *vs.* dijet mass. With 98.7% confidence we observe a peak in the top mass - dijet mass plane. The peak and its projections are similar both in shape and magnitude to expectations based on the decay sequence $t \to bW$, $W \to jj$ for our mixture of top signal and background.

ACKNOWLEDGMENTS

We thank the Fermilab Accelerator, Computing, and Research Divisions, and the support staffs at the collaborating institutions for their contributions to the success of this work. We also acknowledge the support of the U.S. Department of Energy, the U.S. National

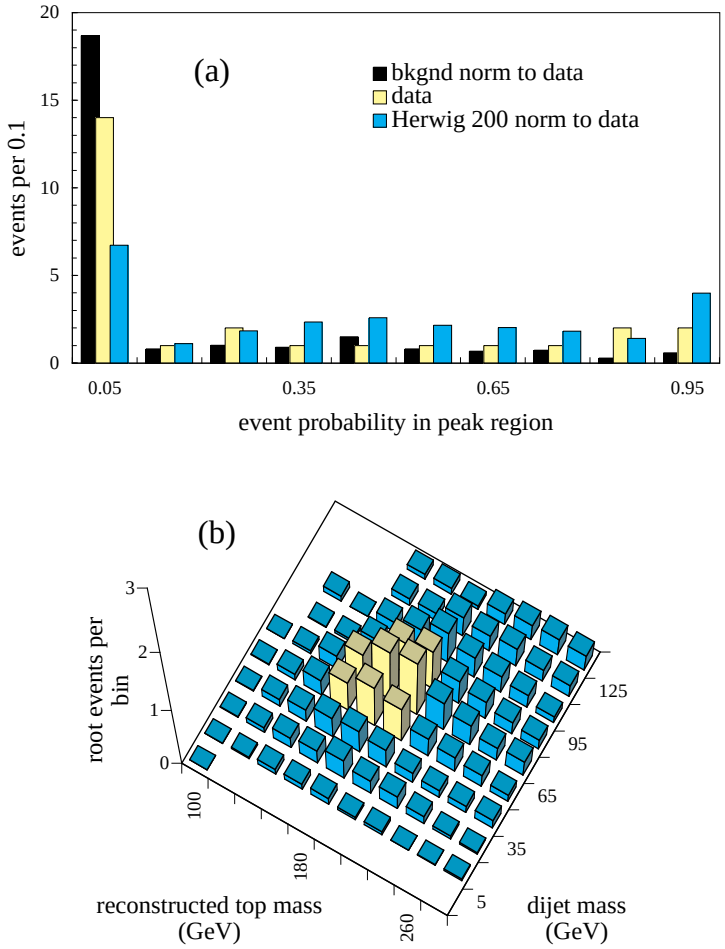

FIG. 11. (a) Distribution of the sum of each event's increments to the peak region of the Lego plot, for (light shaded) data, (medium) HERWIG 200 GeV/c^2 top Monte Carlo, and (black) background events. Monte Carlo and background are normalized to the area of the data (26 events). A binned Poisson-statistics maximum likelihood fit to the shapes of these distributions yields a top fraction of $0.43^{+0.23}_{-0.20}$. Forcing the top fraction to zero decreases the likelihood by an amount corresponding to a gaussian excursion of 2.2 standard deviations (1.3% single-sided probability). (b) Definition of the peak region. Shown is the Lego distribution of HERWIG 200 GeV/c^2 Monte Carlo (HW200) divided by the square root of the sum of HW200 and background. The eight light shaded bins define the peak region used in part (a).

Science Foundation, the Commissariat à L'Energie Atomique in France, the Ministry for Atomic Energy and the Ministry of Science and Technology Policy in Russia, CNPq in Brazil, the Departments of Atomic Energy and Science and Education in India, Colciencias in Colombia, CONACyT in Mexico, the Ministry of Education, Research Foundation and KOSEF in Korea and the A.P. Sloan Foundation.

REFERENCES

1. DØ Collaboration, S. Abachi *et al.*, Phys. Rev. Lett. **74**, 2632 (1995). Ref. (5) fully describes the 2C top mass analysis.
2. DØ Collaboration, J. Bantly *et al.*, *Observation of the Top Quark*, these Proceedings.
3. Our jet calibration method is similar to that described by the CDF Collaboration, F. Abe *et al.*, Phys. Rev. Lett. **69**, 2898 (1992).
4. M. Pang, *Search for Top in $p\bar{p}$ Collisions at $\sqrt{s}$ = 1.8 TeV by Constrained Kinematic Fitting.* Ph.D. thesis, Iowa State University, Ames, Iowa (1994).
5. S. Snyder, *Measurement of the Top Quark Mass at DØ.* Ph.D. thesis, State University of New York, Stony Brook, New York (May 1995).
6. Of each pair of solutions which differ only in neutrino longitudinal momentum, only the more probable solution is allowed to contribute to this average.
7. F. Paige and S. Protopopescu, BNL Report no. BNL38034 (1986, unpublished), release 6.49.
8. F. Carminati *et al.*, *GEANT User's Guide.* CERN Program Library (1991, unpublished).
9. F.A. Berends, H. Kuijf, B. Tausk, and W.T. Giele, Nucl. Phys. **B357**, 32 (1991), release 3.0.
10. G. Marchesini *et al.*, Comput. Phys. Commun. **67**, 465 (1992).
11. CDF Collaboration, F. Abe *et al.*, Phys. Rev. **D50**, 2966 (1994), p. 3020.
12. The masses $m(bjj)$ and $m(bl\nu)$ are weighted 50:50 for e+jets data and 60:40 for μ+jets.
13. We use the CERNLIB program HMCMLL. R. Barlow and C. Beeston, Comput. Phys. Commun. **77**, 219 (1993).